Journal of
Ceramic Science
and Technology

J. Ceram. Sci. Technol., **11** [2] 111-116 (2020)
DOI: 10.4416/JCST2020-00008
available online at: http://www.ceramic-science.com

Short Communication

Improved Direct-Current Aging Stability and Suppressed Leakage Current of Zinc Oxide Varistors by Co-doping with Boron, Gallium, and Yttrium

Kuan Cheng[1], Weiqing Wang[1], Dongji Liu[1], Qingyun Xie[2], Yuanxiang Zhou[3], Hongfeng Zhao[*1]

[1]School of Electrical Engineering, Xinjiang University, Urumqi 830047, China
[2]Xidian Surge Arrester Co., Ltd, Xi'an, Shanxi, 710200, China
[3]State Key Lab of Power Systems, Department of Electrical Engineering, Tsinghua University, Beijing 100084, China

received March 24, 2020; received in revised form June 7, 2020; accepted June 17, 2020

Abstract

The effect of B^{3+}, Ga^{3+} and Y^{3+} co-doping on the microscopic and electrical properties of ZnO varistors is studied. Co-doping with multiple ions greatly improves the comprehensive performance of the ZnO varistors. The doped Ga^{3+} increases the acceptor concentration, raises the barrier height, and inhibits the increase of leakage current. Y^{3+} increases the voltage gradient by limiting the growth of grains. B^{3+} improves the resistance of ZnO varistors to direct-current aging. The varistor with a B^{3+} content of 0.2 mol% achieves a voltage gradient of 450 V/mm, leakage current of 0.54 A/cm^2, and a nonlinear coefficient of 79. Accelerated aging experiments carried out for 1 000 h at 0.9 U_{1mA} and 115 °C give an aging coefficient of 0.027. This research illustrates the ability of cation co-doping to improve the protection effect of metal oxide arrestors and the stability of power systems that operate at ± 1100 kV.

Keywords: Ceramic, varistor, electrical properties, DC aging, aging coefficient

I. Introduction

With the development of economic globalization, the demand for electricity is rapidly increasing. However, the uneven distribution of the world's energy generation and use requires ultra-high voltage (UHV) direct-current (DC) technology for long-distance and large-capacity transmission across regions and countries [1]. The construction of ±1100-kV UHV DC technology raises the requirements for the safe and stable operation of power grids [2]. The arrester plays an irreplaceable role in the safe and stable operation of a power grid, especially in the suppression of operating and lightning overvoltage [3,4]. The varistor is an important part of the arrester that determines the protection performance of arresters [5]. Because of their high non-linearity and energy absorption capacity, zinc oxide (ZnO) varistors are used extensively as surge protectors in power systems [6–8]. In DC power systems, the arrester is constantly subjected to DC bias, which accelerates the aging process of ZnO varistors and seriously lowers their protection performance, posing a severe potential risk to the safe and stable operation of power grids [9,10]. Therefore, it is particularly important to improve the aging stability of DC ZnO varistors. The leakage current of the ZnO varistor directly affects the service life of the arrester, which has potential risks for the safe and stable operation of the power system [11]. Rare earth elements can be introduced to improve the other properties of arrestors, but it is necessary to restrain the increase of leakage current [12]. Doping a ZnO varistor with boron oxide (B_2O_3) improved its stability and suppressed leakage current [13]. However, the co-doping of ZnO varistors with boron (B^{3+}), gallium (Ga^{3+}), and yttrium (Y^{3+}) has not been investigated. In this study, the effects of B^{3+}, Ga^{3+}, and Y^{3+} co-doping on the electrical properties of ZnO varistors are studied in detail.

II. Experimental Procedure

High-performance DC ZnO varistor samples were prepared using the following raw materials: (94-x) mol% ZnO, 1.0 mol% Bi_2O_3, 0.75 mol% MnO_2, 1.0 mol% Co_2O_3, 0.5 mol% Cr_2O_3, 1.0 mol% Sb_2O_3, 1.2 mol% SiO_2, 0.45 mol% Y_2O_3, 0.1 mol% Ga_2O_3, and x mol% B_2O_3 (x = 0.1, 0.2, 0.3, or 0.4 mol%). The mixed raw materials and an appropriate amount of deionized water were placed in a micro-nanopowder dispersion mill to give a ratio of raw materials to water of 2:3. Polyvinyl alcohol (400 mL) and dispersant (150 g) were added and then ball milling was carried out for 11 – 12 h to uniformly disperse the raw materials. The resulting slurry was spray granulated and then the powder was pressed at 400 MPa to form a disk with a diameter of 30 mm and thickness of 2.0 mm. The disks were heated at a rate of 5 °K/min to 1200 °C,

* Corresponding author: zhf_zhf@126.com

sintered for 3 h in a furnace (Nabertherm LH60/14, Germany), and then cooled in air at a rate of 2 °K/min. The surfaces of the sintered varistors were polished, coated with silver paste, and then sintered at 550 °C for 2 h to obtain an electrode. Scanning electron microscopy (SEM; Hitachi 8010, Japan) was used to observe the surface microstructure of the samples [14]. A source meter (Keithley 2410, USA) was used to measure the electric field-current density (*E-J*) relationship of the sample in the pre-breakdown region. The breakdown electric field (E_{1mA}) was measured at $J = 1.0$ mA/cm^2 and the leakage current density (J_L) was measured at a breakdown electric field of 0.75 E_{1mA}. The following formula was used to calculate the non-linear coefficient α: $\alpha = logI_2 - logI_1/(logE_2 - logE_1)$. A broadband dielectric device (Novocontrol Concept 80, Germany) was used to measure the capacitance-voltage (*C-V*) characteristics of the varistors at 1 kHz. X-ray diffraction (XRD; Rigaku H/max 2500, Japan) was used to analyze the crystal phase composition of the varistors.

III. Results and Discussion

Fig. 1 shows an SEM image of varistors with B_2O_3 content of 0.1 – 0.4 mol%. The average particle diameter (*d*) of the ZnO varistors doped with different concentrations of B^{3+} was measured with the linear intercept method and the results are listed in **Table 1**. With increasing B^{3+} concentration, *d* decreased only slightly, indicating that the B^{3+} doping concentration had little effect on the grain size of ZnO.

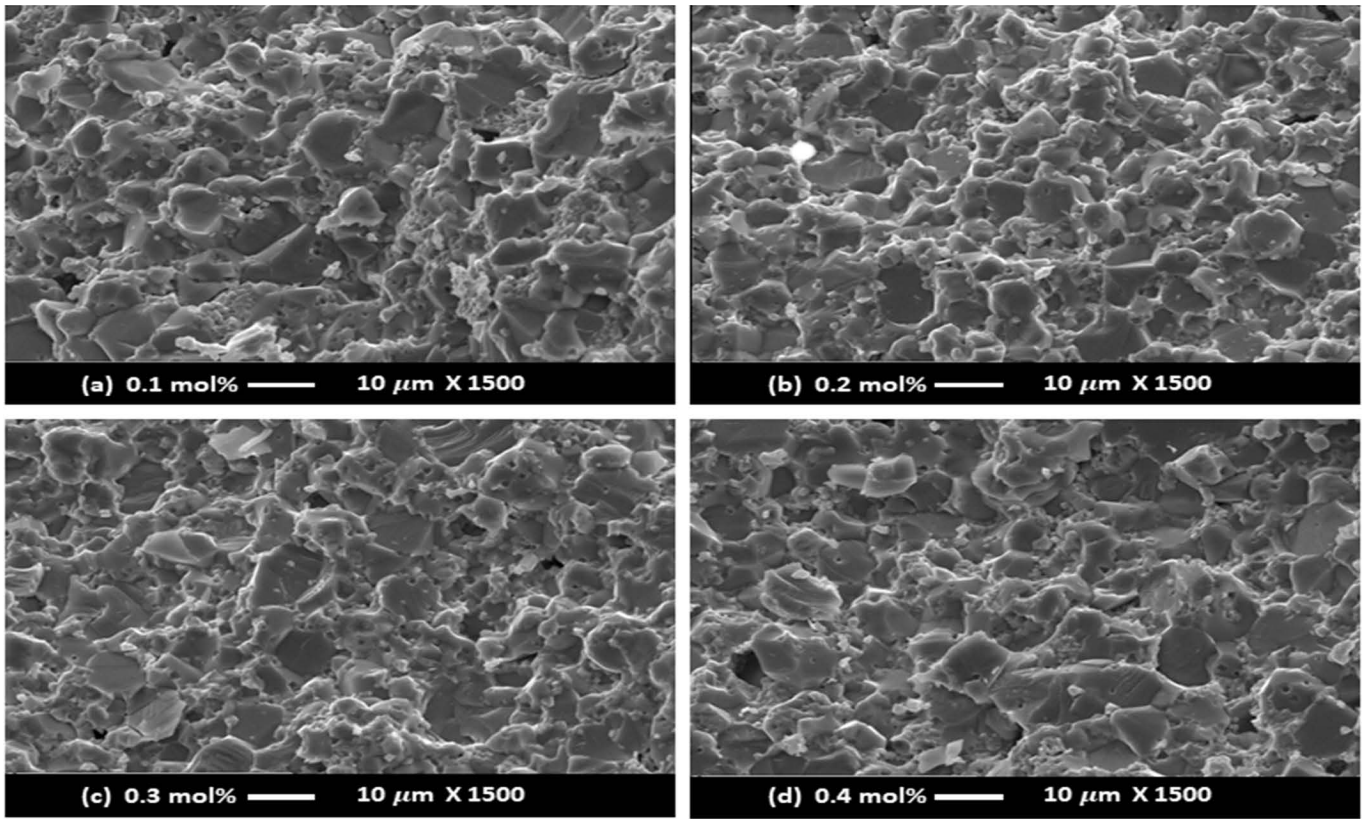

Fig. 1: Scanning electron microscopy images of ZnO varistors prepared with various concentrations of B: (a) 0.1, (b) 0.2, (c) 0.3, and (d) 0.4 mol%.

Table 1: Microstructure, *E-J*, and *C-V* characteristic parameters of samples prepared with various concentrations of B.

B_2O_3 concentration (mol%)	d (μm)	N_d ($\times 10^{23}$ m^{-3})	φ_b (eV)	N_i ($\times 10^{16}$ m^{-2})	E_{1mA}(V/mm)	J_L(μA/cm^2)	α
0.1	6.7	1.5	2.05	1.7	410	1.2	66
0.2	6.5	2.1	2.79	2.4	450	0.54	79
0.3	6.3	1.9	2.38	2.0	438	0.68	73
0.4	6.1	1.6	2.14	1.8	425	0.86	69

The *E-J* characteristics of the ZnO varistors are shown in **Fig. 2**. The parameters calculated from the *E-J* curves, such as E_{1mA}, J_L, and α, are summarized in Table 1. Within the B_2O_3 range of 0.1 to 0.4 mol%, as the B^{3+} doping concentration increased, E_{1mA} and α first increased and then decreased, whereas J_L showed the opposite behavior. When the B_2O_3 doping content was 0.2 mol%, the maximum E_{1mA} of the samples of 450 V/mm was obtained, along with an α of 79 and J_L of 0.54 μA/cm^2. An E_{1mA} value of 450 V/mm is suitable for ± 1100-kV UHV power systems and will allow the size of the arrester to be substantially reduced and its internal structure to be optimized to make the potential distribution more uniform [6, 15]. Suppressing leakage current helps to improve the long-term stability of ZnO arresters [12]. The J_L is lower than the 1 μA/cm^2 required in grid application for continuous running stability [16]. In this paper, the J_L is 0.54 μA/cm^2, which is even lower than that of 1 μA/cm^2, which improved the stability of arrestors greatly, and consequently the operation stability of ± 1 100-kV UHV power systems.

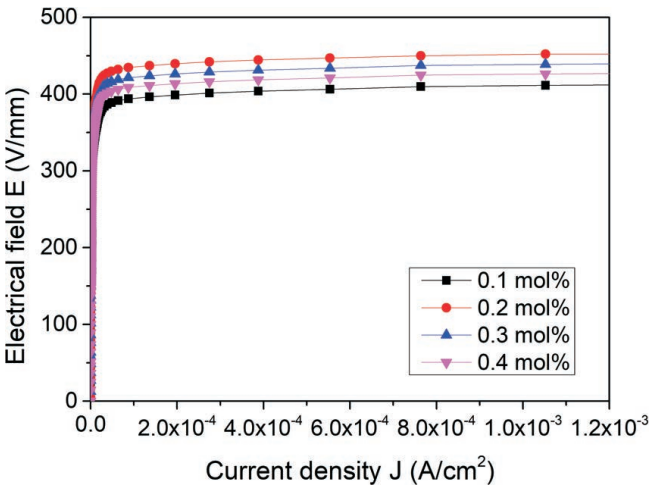

Fig. 2: Current density-electrical field (*E-J*) characteristics of samples with B_2O_3 ranging from 0.1 to 0.4 mol%.

To investigate the Schottky barrier in the ZnO varistors, the voltage dependence of the measured capacitance was measured; the results are shown in **Fig. 3**. The donor concentration N_d, barrier height φ_b, and interface state concentration N_i calculated from the *C-V* curves are summarized in Table 1. These parameters were calculated from the *C-V* equation [17]:

$$\varphi_b = eN_i^2/2N_d\varepsilon\varepsilon_0 \quad (1)$$

Eq. (1) shows that the Schottky barrier is a comprehensive result of the interaction between N_i and N_d at the ZnO grain interface. The maximum potential voltage of 2.79 V was obtained for the ZnO varistor with 0.2 mol% B^{3+}. At finite φ_b, the higher the potential barrier of the ZnO varistor, the greater the E_{1mA}.

It is noteworthy that the trend of φ_b is consistent with that of α, which is opposite to the trend of J_L in Table 1. In the Ga^{3+} doping range of 0.1 to 0.2 mol%, rare-earth Ga^{3+} behaves as a donor ion and affects both N_i and N_d, but the increase of N_i is much larger than that of N_d [18]. Eq. (1) reveals that Ga^{3+} doping increases φ_b of the varistor.

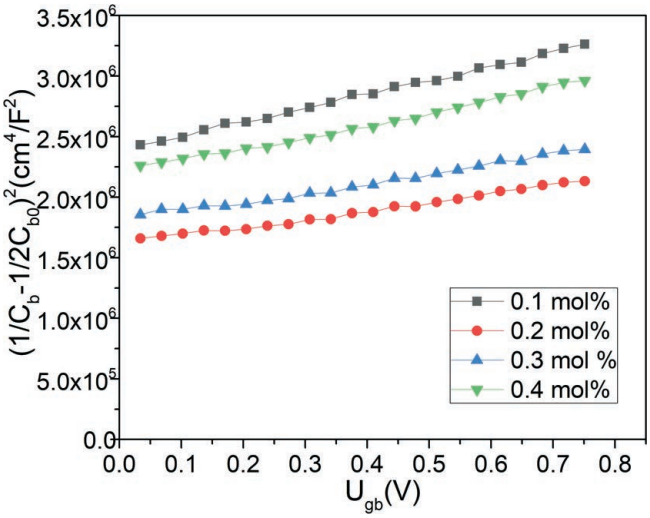

Fig. 3: *C-V* plots of ZnO varistor samples prepared with various concentrations of B.

The liquid-phase sintering time of the ZnO-Bi_2O_3 system can be prolonged by the low melting point of B_2O_3 (450 °C) [9], which promotes ion exchange between ZnO grains and other additives at grain boundaries, allowing more Ga^{3+} to enter the grains and further raise φ_b. The increase of φ_b inhibits the increase of leakage current [16]. The nonlinear effect of ZnO varistors is controlled by the φ_b [4]. Therefore, an increase in φ_b contributes to an increase of α. The increase of α is beneficial to improve the protection properties of arrestors under all kinds of impulse current, so the operational stability of the grid is improved. Within the B^{3+} concentration range of 0.2 to 0.4 mol%, α and E_{1mA} decreased with increasing B_2O_3 content, as shown in Table 1. Rare-earth Y^{3+} mainly existed at grain boundaries to form the spinel phase, which limited the growth of ZnO grains through pinning effect and enhanced E_{1mA} [19]. Meanwhile, the effect of Y^{3+} on N_d is greater than that on N_i, which can decrease the φ_b and increase J_L [18]. With increasing B_2O_3 content of the raw materials, the liquid-assisted sintering process became more effective. Because the Y^{3+} doping content was higher than that of Ga^{3+}, more Y^{3+} than Ga^{3+} can dissolve into the ZnO particles, which decreases the thickness of the barrier layer. The decrease of φ_b leads to decreases of E_{1mA} and α and the increase of J_L.

To determine the stability of the co-doped ZnO varistors in a UHV DC transmission system, an accelerated aging test for 1 000 h at 0.9 E_{1mA} and 115 °C was used to verify the DC anti-aging performance of the varistor doped with 0.2 mol% B^{3+}. The results of the aging test are shown in **Fig. 4**. The DC accelerated aging curve rapidly increased to the maximum power loss and then slowly decreased. After a DC voltage had been applied for about 45 h, the curve began to flatten. The gentle aging curve indicated that the power loss of the sample was stable. The sample operated for a long time without thermal collapse at a working voltage of 0.9 E_{1mA}. In an evaluation of the aging properties of varistors, the degradation rate coefficient (K_t) is usually determined using the following equation:

$$K_t = \frac{I_L - I_{L0}}{\sqrt{t}} \quad (2)$$

where I_{L0} is the leakage current at $T = 0$. A lower K_t indicates a varistor has higher stability. K_t calculated for the ZnO varistor doped with 0.2 mol% B^{3+} is 0.027. This value indicated that B^{3+} doping greatly improved the aging resistance of DC ZnO varistors. Because the ionic radius of B^{3+} is 0.027 nm smaller than that of a zinc ion (Zn^{2+}; 0.074 nm), a small amount of B^{3+} can penetrate into the ZnO grains and occupy the interstitial position, which reduces the concentration of interstitial Zn^{2+} [20,21]. B^{3+} doped into the ZnO crystals during the high-temperature sintering process formed a glass phase at the grain boundary, which decreased the content of grain boundary defects, effectively inhibiting the migration of interstitial Zn ions and suppressing the distortion of the Schottky barrier [22]. The prepared samples can further lower the Zn^{2+} concentration in the gap by means of high-temperature heat treatment [20]. The defect reactions can be expressed by the following equations [20]:

$$V_O^X O + O = O_O^X \quad (3)$$

$$O_O^X + V_{Zn}^- = O_O^{X-} + V_{Zn}^X \quad (4)$$

$$Zn_i^+ + V_{Zn}^X = V_i^X + Zn_{Zn}^+ \quad (5)$$

$$Zn_{Zn}^+ + O_O^- = ZnO \quad (6)$$

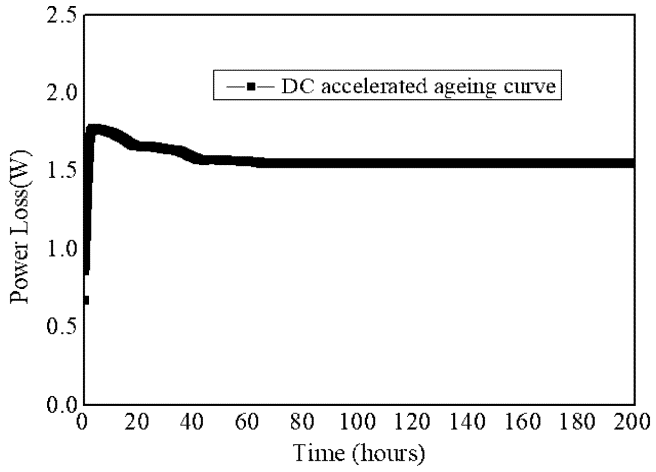

Fig. 4: DC acceleration aging curve of a typical sample doped with 0.2 mol% boron.

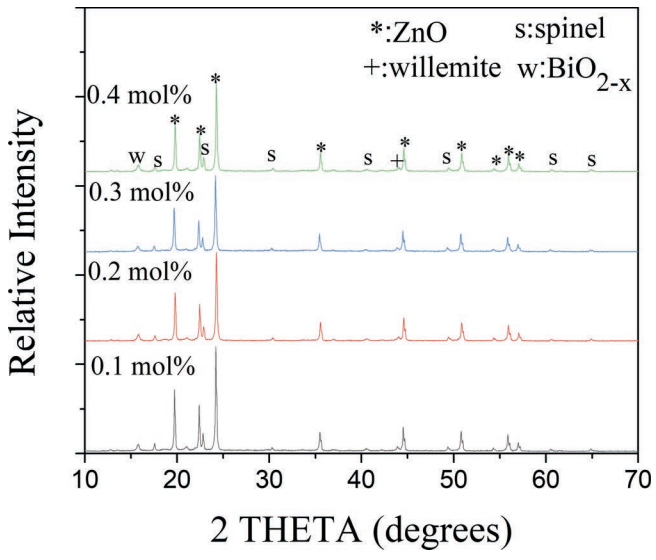

Fig. 5: X-ray diffraction patterns of ZnO varistor samples prepared with various concentrations of B co-dopant.

The XRD patterns of ZnO varistor samples doped with different B^{3+} content are shown in **Fig. 5**. The patterns indicated that the varistors mainly contained ZnO, spinel, willemite, Bi_2O_3, and BiO_{2-x} phases. Only a small amount of willemite (h = 56.004, d = 1.6406 nm) was observed in the XRD patterns. No new phases were observed, and the peak intensity was low because of the small amount of B^{3+} doped in the samples.

IV. Conclusions

DC ZnO varistors with co-doped B^{3+}, Ga^{3+}, and Y^{3+} were fabricated. These varistors displayed a high gradient, low leakage, and strong DC aging resistance. The ZnO varistor with a B^{3+} content of 0.2 mol% displayed the highest performance of the varistors studied, with an E_{1mA} of 450 V/mm, α of 79, J_L of 0.54 A/cm^2, and K_t of 0.027. The high E_{1mA}, small J_L, high non-linearity, and stable aging performance of the DC ZnO varistor studied in this paper is of great significance for the safe and stable operation of ± 1100-kV UHV power systems.

Acknowledgments

This work was supported by the Shanghai Cooperation Organization Science and Technology Partnership Program (grant number 2017E01015)

References

1 Arcia-Garibaldi, G., Cruz-Romero, P., Gómez-Expósito, A.: Future power transmission: visions, technologies and challenges, *Renew. Sustain. Energy. Rev.*, **94**, 285 – 301, (2018).

2 Liu, Z.H., Zhang, F.X., Yu, J., Gao, K.L., Ma, W.M.: Research on key technologies in ±1100 kV ultra-high voltage DC transmission, *High Volt.*, **3**, 279 – 288, (2018).

3 Clarke, D.R.: Varistor ceramics, *J. Am. Ceram. Soc.*, **82**, 485 – 502, (1999).

4 Liu, F., Xu, G., Duan, L., Li, Y., Li, Y., Cui, P.: Influence of B_2O_3 additives on microstructure and electrical properties of ZnO-Bi_2O_3-Sb_2O_3-based varistors, *J. Alloy. Compd.*, **509**, 56 – 58, (2011).

5 Gupta, T.K.: Effect of minor doping on the high current application of the ZnO varistor, *Ferroelectrics*, **102**, 391 – 396, (1990).

6 Imai, T., Udagawa, T., Ando, H., Tanno, Y., Kayano, Y., Kan, M.: Development of high gradient zinc oxide nonlinear resistors and their application to surge arresters, *IEEE. T. Power. Del.*, **13**, [4], 1182 – 1187, (1998).

7 Chen, Q.H., He, J.L., Tan, K.X., Chen, S.M., Yan, M.Y.: Influence of grain size on distribution of temperature and thermal stress in ZnO varistor ceramics, *J. Sci. China Ser.*, **E45**, [4], 337 – 347, (2002).

8 Gupta, T.K.: Application of zinc oxide varistors, *J. Am. Ceram. Soc.*, **73**, 1817 – 1840, (1990).

9 Cheng, L.H., Li, G.R., Yuan, K.Y., Meng, L., Zheng, L.Y.: Improvement in nonlinear properties and electrical stability of ZnO varistors with B_2O_3 additives by nano-coating method, *J. Am. Ceram. Soc.*, **95**, 1004 – 1010, (2011).

10 Li, C.Y., Lin, C.J., Yang, Y., Zhang, B., Liu, W.D., Li, Q., Hu, J., He, S., Liu, X.L., He, J.L.: Novel HVDC spacers by adaptively controlling surface charges – Part II: Experiment, *IEEE Trans. Dielectr. Electr. Insul.*, **25**, [4], 1248 – 1258, (2018).

11 Zhao, H.F., He, J.L., Hu, J., Chen, S.M., Xie, Q.Y.: High nonlinearity and low residual-voltage ZnO varistor ceramics

by synchronously doping Ga_2O_3 and Al_2O_3, *J. Mater. Lett.*, **164**, [1], 80 – 83, (2016).

12 He, J.L., Liu, J., Hu, J., Long, W.C.: AC ageing characteristics of Y_2O_3-doped ZnO varistors with high voltage gradient, *J. Mater. Lett.*, **65**, [17], 2595 – 2597, (2011).

13 Jiang, S.L., Xie, T.T., Zhang, H.B., Guo, T., Huang, Y.Q.: Study on the ZnO-Based ceramic films for low-voltage varistors with high stability, *J. Electroceram.*, **21**, [21], 528 – 531, (2008).

14 Wurst, J.C., Nelson, J.A.: Lineal intercept technique for measuring grain size in two-phase polycrystalline ceramics, *J. Am. Ceram. Soc.*, **55**, [2], 109 – 111, (1972).

15 He, J.L., Hu, J., Lin, Y.H.: High voltage gradient ZnO varistor ceramics with rare earth dopants, *J. Sci. China Ser.*, **E39**, 109 – 113, (2009).

16 Zhao, H.F., He, J.L., Hu, J., Chen, S.M., Xie, Q.Y.: High nonlinearity and high voltage gradient ZnO varistor ceramics tailored by combining Ga_2O_3, Al_2O_3, and Y_2O_3 dopants, *J. Am. Ceram.*, **99**, [3], 769 – 772, (2016).

17 Gupta, T.K., Carlson, W.G.: A grain-boundary defect model for instability/stability of a ZnO varistor, *J. Mater. Sci.*, **20**, 3487 – 3500, (1985)

18 Gupta, T.K.: Microstructural engineering through donor and acceptor doping in the grain and grain boundary of a polycrystalline semiconducting ceramic, *J. Mater. Res.*, **7**, [12], 3280 – 3295, (1992).

19 Bernik, S., MačEk, S., Ai, B.: The characteristics of ZnO-Bi_2O_3-Based varistor ceramics doped with Y_2O_3 and varying amounts of Sb_2O_3, *J. Eur. Ceram. Soc.*, **24**, 1195 – 1198, (2004).

20 He, J.L., Zeng, R., Tu, Y.P., Han, S.W., Cho, H.G.: Aging characteristics and mechanisms of ZnO nonlinear varistors, in: Proceedings of the 6th International Conference on Properties and Applications of Dielectric Materials, June 21 – 26, 2000, Xi'an, China.

21 Eda, K., Iga, A., Matsuoka, M.: Degradation mechanism of non-ohmic zinc oxide ceramics, *J. Appl. Phys.*, **51**, [5], 2678 – 2684, (1980).

22 Glot, A.B., Mazurik, S.V.: Nonlinear electrical properties of zinc oxide ceramics with B_2O_3 additions, *Inorg. Mater.*, **36**, [6], 636 – 639, (2000).